Denoising of Radar Pulse Streams With Autoencoders

Xueqiong Li, Zhang-Meng Liu, and Zhitao Huang

***Abstract*— There are many cases in which the noise corrupts the signals in a significant manner. To better analyze these signals, the noise must be removed from the signals for further data analysis, and the process of noise removal is referred to as denoising. In this letter, we propose a novel approach to the pulse denoising problem by extracting features from time of arrival (TOA) sequences using the autoencoders. The noise-contaminated TOA sequence is first coded into a binary vector and then fed into an autoencoder for training. Then, the trained autoencoder is capable of generating the original TOA sequence without lost and spurious pulses. Moreover, the proposed method does not require a noise-free TOA sequence as a priori as with conventional autoencoders. Simulation results show that the new technique can deal with TOA sequences with complex pulse repetition interval (PRI) modes that have not been tackled before. In addition, the proposed method has a better performance in noisy environments than conventional methods and general deep neural network structures.**

***Index Terms*— Denoising, pulse streams, TOA sequences, autoencoders, binary coding.**

I. Introduction

THE problem of noise removal has received a great interest in various fields such as signal processing [1], [2], image processing [3], [4], and video processing [5], [6]. The noise corrupts the signals in a significant manner, and it must be removed from the data in order to proceed with further data analysis. The process of noise removal is generally referred to as signal denoising.

The goal of signal denoising is to remove noise and meanwhile to preserve the essential signal structure. To the best of our knowledge, most signal denoising methods are performed on the original signal. Wavelet transform (WT) [7]–[9] and empirical mode decomposition (EMD) [10], [11] are the mainstream methods of signal denoising [12]. However, the radar signal is always in the form of pulses which are measured by several statistical features. Therefore, the following tasks such as denoising, deinterleaving and classification are performed using these numerical features and the conventional denoising methods can no longer be used.

Time of arrival (TOA) is a feature of the pulse description words (PDWs) used as a measurement parameter of radar pulse streams. The first difference of a TOA sequence is called pulse repetition interval (PRI). PRI represents the periodicity of the pulse streams, which is the most reliable and stable parameter of PDWs and has been used to categorize and analyze various emitters over time [13]–[16]. Therefore, the noise-free TOA sequences are of great value for emitter identification, and TOA sequence denoising is a very important task.

In this letter, the autoencoder is introduced to perform TOA sequence denoising. An autoencoder is an unsupervised artificial neural network originally used to learn the efficient representations of the input. In the past few years, the autoencoders have been widely applied in many fields. Noh *et al.* [17] use convolution and deconvolution layers as autoencoder to perform semantic segmentation. Yang *et al.* [18] develop an autoencoder architecture to generate images. Rasmus *et al.* [19] use a denoising autoencoder architecture for unsupervised and semi-supervised feature learning. Rematas *et al.* [20] present an autoencoder architecture for reflectance maps prediction of objects. These successful applications indicate that the autoencoders are capable of learning the inherent regularity of the input data. Therefore, it is feasible to use the autoencoders for TOA denoising, which attempt to extract the intrinsic PRI modes from the noise-contaminated TOA sequences.

With the above motivations, a learning-based TOA denoising framework is introduced in this letter to handle TOA sequence denoising problems. The noise-contaminated TOA sequence is first coded as a binary vector and then fed into an autoencoder. We also use them as the target of the autoencoder. The proposed autoencoders can automatically learn the inherent PRI regularity of the input pulse streams. After the training phase, a reconstructed noise-free TOA sequence is generated. Statistical simulation results demonstrate that the denoising performance is satisfactory despite of high ratio of lost and spurious pulses.

Compared with other existing methods, this letter has the following innovations. First, an end-to-end pulse denoising framework is established through unsupervised learning. It differs from the traditional pulse denoising methods in that it seeks the inherent regularity of the TOA sequence rather than the original signals. Second, the input sequence is binary coded to allow the autoencoders to better understand and analyze the TOA sequence, which has superior performance than using the original TOA sequence as the input. Third, the proposed denoising scheme successfully adapts the autoencoder, originally designed for the feature learning, to the task of TOA denoising. It is different from the conventional denoising autoencoders because it does not require the noise-free data as a target. Hence, this work is different from the traditional denoising methods and the basic autoencoders, and can achieve satisfying performance at a high noise ratio.

Manuscript received December 12, 2019; revised January 13, 2020; accepted January 13, 2020. Date of publication January 22, 2020; date of current version April 9, 2020. This work was supported by the Program for Innovative Research Groups of the Hunan Provincial Natural Science Foundation of China under Grant 2019JJ10004. The associate editor coordinating the review of this letter and approving it for publication was M. Chafii. *(Corresponding author: Xueqiong Li.)*

The authors are with the Department of Electronic Science, National University of Defense Technology, Changsha 410073, China (e-mail: lixueqiong13@nudt.edu.cn).

Digital Object Identifier 10.1109/LCOMM.2020.2967365

II. Problem Formulation

In this section, we address the mathematical formulation of TOA denoising. The TOA sequence of the pulse streams can be written as $T = \{t_1, t_2, \ldots, t_N\}$, where t_i is the ith pulse of the stream and N is the number of the intercepted pulse.The first difference of TOA sequence shows the inherent regularity of TOA sequences, which is presented as PRI: $P = \{p_1, p_2, \ldots, p_{N-1}\}, p_i = t_{i+1} - t_i$.

Four types of PRI modulations are considered in this letter, namely the constant PRI, sliding PRI, dwell and switch (D&S) PRI and wobulated PRI. These four types of PRI sequences can be described as follows [21].

Constant PRI: A constant PRI sequence always has a fixed value of k. $p_n = k, \forall n \in \mathbb{Z}+$ for some real number $k > 0$.

Sliding PRI: $p_n = PRI_0 + \delta * (n \bmod M)$ where $PRI_0 > 0$ is the initial PRI value of a sliding period, $\delta \in \mathbb{R}$ is some value indicating the rate of change in PRI during a sliding period and M is the number of pulses in each sliding window.

Dwell and Switch (D&S) PRI: There are several stable values in the D&S PRI sequence, but the values remain at the same value $y_i > 0 \forall i$ for several pulses $x_i - x_{i-1}$ before switching to another value $y_{i+1} > 0$ in the D&S PRI.

Wobulated PRI: The values of wobulated PRI sequence always have a shape similar to the sinusoidal function, and also appear periodically. $p_n = PRI_0 + A \sin(\omega * x_n + \varphi)$ where $PRI_0 > 0$ is the value that PRI will oscillate around. A is the amplitude of the modulation, ω is the frequency of the sine function, φ is the phase of the sine function, and x_n is some value proportional to n defining the sampling resolution.

Although the regularity of the above TOA sequences seems to be easily recognized in an ideal environment, the noise in real electronic warfare environment makes it a rather difficult problem. There are two kinds of noise considered in this letter. These noises destroy the PRI patterns and breaks the regularity of the sequences. In this letter, noise ratio indicates the ratio of noise to the entire sequence.

1) Lost Pulses: There are some pulses missing during receiving the signals and it happens randomly. When there are j pulses lost from the ith pulse to $(i + j - 1)$th pulse in the received TOA sequence, then the new PRI sequence P_1 can be represent as:

$$P_1 = \begin{cases} p_n, & n = 1, 2, \ldots, i-2 \\ p_{i-1} + \ldots + p_{i+j-1}, & n = i-1 \\ p_{n+j}, & n = i, \ldots, N-j-1. \end{cases} \quad (1)$$

2) Spurious Pulses: The received spurious pulses are emitted by other emitters, and they will break the regularity of the original pulse streams which also happen randomly. If there are j pulses attached to the ith pulse which have the first difference as $g_k = \{g_0, g_1, \ldots, g_j\}$, then the new PRI sequence P_2 can be described as:

$$P_2 = \begin{cases} p_n, & n = 1, 2, \ldots, i-1 \\ g_{n-i}, & n = i, \ldots, i+j \\ p_{n+j}, & n = i+j+1, \ldots, N+j-1, \end{cases} \quad (2)$$

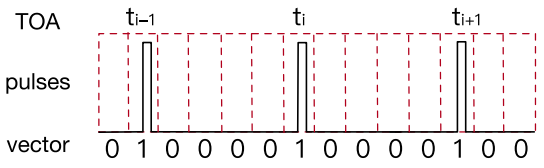

Fig. 1. The TOA sequence is converted into a vector consisting of ones and zeros.

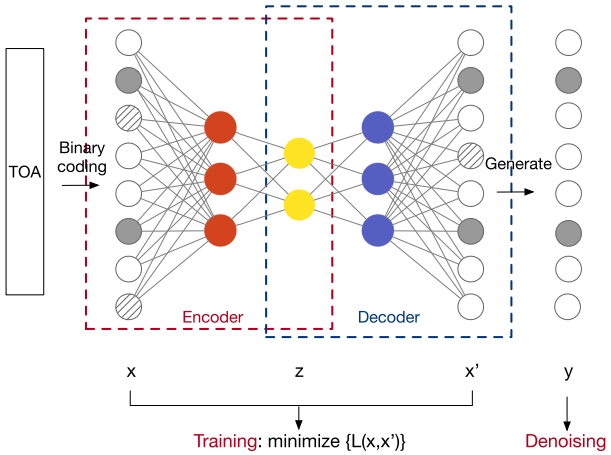

Fig. 2. The structure of the denoising model. The binary coded TOA sequences are fed into the autoencoder as the input and target. To minimize the loss between the output and target, a new representation of the TOA sequences without noise is generated.

where j is the number of inserted pulses. g_0 and g_j are the differences between the original pulse and the spurious pulse. g_1 to g_{j-1} is the difference between the spurious pulses themselves.

III. The Proposed Denoising Model

A. Representation of TOA Sequence

The TOA sequences are first coded into binary vectors to be compatible with modern deep learning models. The original TOA sequence $T = \{t_1, t_2, ...t_N\}$ is converted into a vector consisting of ones and zeros, where each element of the vector corresponds to a time window. Ones in the vector indicate there are some signals received during the corresponding time window, and zeros represent those time windows where no signal or noise was received, as shown in Fig. 1.

B. The Structure of the Proposed Denoising Scheme Based on Autoencoders

The basic principle of the proposed model is to treat the denoising problem as a fitting problem. We make the noise-contaminated TOA sequences as both the input and the target of the autoencoders, and train the autoencoders till the loss among these sequences to a minimum value for each batch. In this way, the purpose of the model is to find a TOA sequence which make the losses minimum. As there are a large amount of TOA sequences are fed into the autoencoders with random noise, the unique optimal solution for this fitting problem is the noise-free TOA sequence. The detailed autoencoder structure is shown in Fig. 2.

As shown in Fig. 2, the proposed autoencoder consists of two parts, namely the encoder and the decoder. Both the encoder and the decoder are composed of several dense layers, and each dense layer can be described as:

$$f(\mathbf{x}) = \sigma(\mathbf{W}\mathbf{x} + \mathbf{b}), \tag{3}$$

where $\mathbf{W}$ represents the weight matrix and $\mathbf{b}$ is the bias vector. σ is the activation function, generally using a nonlinear function.

The encoder stage takes the binary coded TOA sequences $\mathbf{x}$ as the input and maps it to the hidden layer with $\mathbf{z}$:

$$\mathbf{z} = f^{(L)}(\mathbf{x}) = f(\underbrace{\cdots}_{L}(f(\mathbf{x})), \tag{4}$$

where L represents the number of the dense layers of the encoder stage. The output $\mathbf{z}$ of the encoder has a lower dimension than the input in order to learn a "compressed" regularity of the input to ignore unwanted noise. In the decoder stage, $\mathbf{z}$ is mapped to the reconstruction $\mathbf{x}'$ of the same shape as $\mathbf{x}$:

$$\mathbf{x}' = f'^{(L')}(\mathbf{z}) = f'(\underbrace{\cdots}_{L'}(f'(\mathbf{z})), \tag{5}$$

where L' represents the number of the dense layers of the decoder stage.

A sigmoid function is executed at the end of the decoder to ensure that the values of the output vectors are decimals between 0 and 1. However, in our presentation of pulse streams, only zeros and ones have specific physical meanings. Therefore, a threshold τ is set to convert all the output decimals into 0 or 1:

$$y_i = \begin{cases} 0, & x_i{}' < \tau \\ 1, & otherwise, \end{cases} \tag{6}$$

where $x_i{}'$ is the elements of the direct output vectors of the autoencoders, and y_i is the elements of the new vectors after the threshold function.

C. Training of the Denoising Autoencoders

After the proposed model is built, it should be trained till convergence and all parameters of the model should be adjusted. The purpose of training the autoencoder is to minimize the difference between the output and the target. As both the input $\mathbf{x}$ and the output $\mathbf{x}'$ are binary coded TOA sequences, binary cross entropy is used as the loss function in this structure as

$$\begin{aligned} \mathcal{L}(\mathbf{x}, \mathbf{x}') &= \{l_1, \ldots, l_N\}^T, \\ l_n &= -\omega_n[x_n{}' \cdot \log x_n + (1 - x_n{}') \cdot \log(1 - x_n)]. \end{aligned} \tag{7}$$

Here, N_n is the batch size during training process, and ω_n is a weight of different batch.

Before the training begins, all elements of the weight matrices and bias vectors are randomly initialized to decimals between 0 and 1. The training process is carried out according to Eq. (4), (5) and (7) each time a batch of data arrive. The purpose of the training phase is to find the corresponding parameters which minimize the sum of the difference between the output and the target of the entire batch as

$$\mathbf{W}, \mathbf{b} = \arg\min \sum_{i=1}^{N} l_n, \tag{8}$$

where l_n is described in Eq. (7).

Back-propagation is used to tune the parameters of the model during training phase as

$$\alpha_{new} = \alpha_{old} - \eta \frac{\partial l_n}{\partial \alpha}, \tag{9}$$

where α represents a specific tunable parameter and η is the learning rate.

When the autoencoder converges and all parameters are set, the test TOA sequences can be put into the trained autoencoder for denoising. The trained autoencoder is ideally capable of generating raw TOA sequences without noise.

TABLE I
PRI VALUES OF SIMULATED TOA SEQUENCES

No.	PRI modulation	PRI values (μs)
1	Constant	200
2	Sliding	$\{100, 150, 200, 250, 300\}$
3	D&S	$\{110 * 6, 190 * 6, 320 * 6\}$
4	Wobulated	$p = 150\sin(\frac{\pi}{15}t) + 200$

IV. SIMULATIONS AND ANALYSIS

The detailed autoencoder structure and the environment parameters are introduced in this section and the experiment results are also shown below.

A. Simulation Settings

1) Parameters of TOA Sequences: Four TOA sequences with different PRI modulation modes are tested in this letter, with their PRI values listed in Table I.

During the training phase, for each TOA sequence, there are $\rho_l \in [0, 70\%]$ of the pulses are missing as lost pulses, and $\rho_s \in [0, 50\%]$ of noise are added randomly to the pulse streams as spurious pulses. In addition, during the binary coding phase, the time window is set to $10\mu s$ and there are approximately 150 pulses remain for training.

2) Parameters of the Autoencoders: For the denoising of TOA sequences with four different PRI modulation modes, four autoencoders are constructed. These autoencoders have the same structure to illustrate the robustness to different PRI modulation modes. $10,000$ TOA samples with 300 pulses are first converted to binary vectors with length of 1500, and then fed into the autoencoder for each modulation modes with batch size of 64. The learning rate is set $\eta = 0.001$ and the weight decay is 1×10^{-5}. The output vector has the same size with the input vector. The parameters of the encoder and the decoder are described as follows.

Encoder: The encoder is composed of three fully connected layers with neuron numbers of 128, 64 and 32. Rectified linear units (ReLU) is followed by each fully connected layer to make sure a non-linear process.

TABLE II
THE DENOISING RESULTS OF FOUR TYPES OF TOA SEQUENCES

Lost pulse ratio	Constant				Sliding				D&S				Wobulated			
	10%		70%		10%		70%		10%		70%		10%		70%	
	Pre	Rec	Pre	Rec	Pre	Rec	Pre	Rec	Pre	Rec	Pre	Rec	Pre	Rec	Prec	Rec
0	100	100	100	100	100	100	100	100	100	100	100	100	99.86	96.79	98.40	97.67
10%	100	100	100	100	100	100	100	100	100	100	100	100	99.69	94.58	98.33	96.92
20%	100	100	100	100	100	100	100	100	100	99.97	100	100	99.92	91.86	98.25	94.67
30%	100	99.61	100	100	100	97.58	100	99.81	100	99.08	100	99.91	99.97	85.49	98.90	92.95
40%	100	89.13	100	93.98	100	75.63	100	89.91	100	83.70	100	90.44	99.96	67.70	99.45	63.71

Decoder: The decoder consists of three fully connected layers with 32, 64 and 128 as the number of neurons and ReLU is followed by each layer.

The proposed model is trained on Pytorch [22] platform. In general, the autoencoder can converge within 15 epochs.

B. Results and Analysis

Experiment 1: The first simulation is carried out by considering the denoising performance of TOA sequences with four types of PRI modes to display the effectiveness of the autoencoder intuitively. As we mentioned before, the results of the output vector consists of zeros and ones, and the ones indicate the locations of real pulses and noise. In this way, the denoising performance is evaluated in terms of $precision$ and $recall$ with different ratio of the lost and spurious pulses. $Precision$ is the ratio of the correctly pulse detected number to the actually pulse detected number. $Recall$ refers to the ratio of the correctly pulses detected number to the real pulse number. In this simulation, the spurious pulses ratio is set to a fixed value as 10% and 70%, and the lost pulse ratio ρ_l is varying from 0% to 40%. The obtained $precision$ and $recall$ are shown in Table II.

The results in Table II demonstrate the robustness of the proposed model to the denoising performance of the four TOA sequences. The wobulated PRI is the most difficult to denoise since its PRI values are more complex than other PRI patterns. Most of $precision$ are 100% while $recall$ is often smaller than $presicion$, because there are still several pulses that are not detected correctly at high noise ratio. In addition, the $recall$ of $\rho_s = 70\%$ is always greater than $recall$ of $\rho_s = 10\%$, this is because when the ratio of noise to the entire sequence is larger, the proportion of the real pulse is lower, so it is easier to choose the right pulses.

Experiment 2: In this experiment, we compare the statistical performance of a conventional method, a general deep neural network (DNN) and the proposed method at different lost and spurious pulse ratios. The conventional method uses the cumulative difference histogram (CDIF) [14] to find the intrinsic PRI values and try to reconstruct the original pulses. The DNN has the same number of layers as the autoencoder, while the number of neurons in each layers is 128. Since the conventional method cannot handle complex PRI modes, sliding PRI is taken as an example of comparison with $\rho_s = 70\%$ and ρ_l ranges from 0 to 50%. $Recall$ is used here to measure the performance of denoising the TOA sequence of sliding PRI mode. The results are shown in Fig. 3.

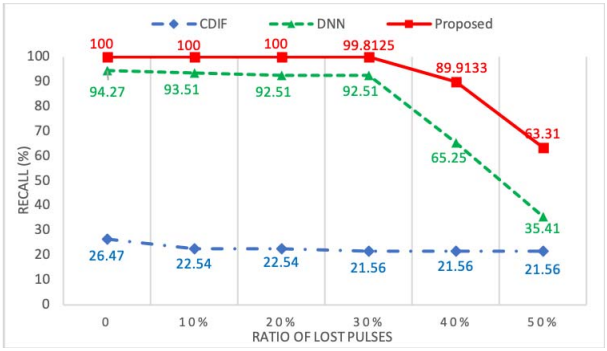

Fig. 3. Performance comparison of denoising the TOA sequence of sliding PRI mode.

The exceeding performance can be seen from Fig. 3. When the spurious pulse ratio $\rho_s = 70\%$, the conventional CDIF method can hardly find the PRI values of the TOA sequences because the spurious pulses have destroyed the PRI regularity, and the histogram of the difference of the TOA sequences is no longer an accurate PRI value. DNN can also be applied in denoising because of the similar characteristic to the autoencoders. However, without using lower dimensional layers to extract the inherent regularity and ignoring noise, the DNN structure has lower performance than the proposed autoencoders, especially when the lost pulse ratio is high. Accordingly, our proposed method has better performance than the traditional method. Also, the autoencoder structure has proven its value in denoising for TOA sequences.

V. CONCLUSION

In this letter, the problem of radar pulse stream denoising is addressed by learning the PRI regularity of noise-contaminated TOA sequences. A denoising autoencoder scheme is proposed to solve this problem, which binary coding the TOA sequences and take them as the input and the target. By minimizing the sum of the losses among these vectors, the raw TOA sequences without noise are generated based on the autoencoders. In the simulation experiments, the autoencoder model shows a great deal of superiority in all the considered scenarios with high ratio of noise. In addition, this model has better performance than conventional methods and general DNN structure. This work can help the further analysis and identify of the radar emitters. Future works may include complex pattern denoising and deinterleaving.

REFERENCES

[1] M. Blanco-Velasco, B. Weng, and K. E. Barner, "ECG signal denoising and baseline wander correction based on the empirical mode decomposition," *Comput. Biol. Med.*, vol. 38, no. 1, pp. 1–13, Jan. 2008.

[2] W. Liu, N. Wang, M. Jin, and H. Xu, "Denoising detection for the generalized spatial modulation system using sparse property," *IEEE Commun. Lett.*, vol. 18, no. 1, pp. 22–25, Jan. 2014.

[3] A. Buades, B. Coll, and J.-M. Morel, "A non-local algorithm for image denoising," in *Proc. IEEE Comput. Soc. Conf. Comput. Vis. Pattern Recognit. (CVPR)*, vol. 2, Jul. 2005, pp. 60–65.

[4] G. Gilboa, N. Sochen, and Y. Zeevi, "Image enhancement and denoising by complex diffusion processes," *IEEE Trans. Pattern Anal. Mach. Intell.*, vol. 26, no. 8, pp. 1020–1036, Aug. 2004.

[5] K. Dabov, A. Foi, and K. Egiazarian, "Video denoising by sparse 3D transform-domain collaborative filtering," in *Proc. 15th Eur. Signal Process. Conf.*, Oct. 2007, pp. 145–149.

[6] L. Jovanov *et al.*, "Combined wavelet-domain and motion-compensated video denoising based on video codec motion estimation methods," *IEEE Trans. Circuits Syst. Video Technol.*, vol. 19, no. 3, pp. 417–421, Mar. 2009.

[7] I. Daubechies, "The wavelet transform, time-frequency localization and signal analysis," *IEEE Trans. Inf. Theory*, vol. 36, no. 5, pp. 961–1005, Sep. 1990.

[8] I. W. Selesnick, R. G. Baraniuk, and N. C. Kingsbury, "The dual-tree complex wavelet transform," *IEEE Signal Process. Mag.*, vol. 22, no. 6, pp. 123–151, Nov. 2005.

[9] S. Baig, U. Ali, H. M. Asif, A. A. Khan, and S. Mumtaz, "Closed-form BER expression for Fourier and wavelet transform-based pulse-shaped data in downlink NOMA," *IEEE Commun. Lett.*, vol. 23, no. 4, pp. 592–595, Apr. 2019.

[10] P. Flandrin, G. Rilling, and P. Goncalves, "Empirical mode decomposition as a filter bank," *IEEE Signal Process. Lett.*, vol. 11, no. 2, pp. 112–114, Feb. 2004.

[11] M. E. Torres, M. A. Colominas, G. Schlotthauer, and P. Flandrin, "A complete ensemble empirical mode decomposition with adaptive noise," in *Proc. IEEE Int. Conf. Acoust., Speech Signal Process. (ICASSP)*, May 2011, pp. 4144–4147.

[12] X. Li, J. Jin, Y. Shen, and Y. Liu, "Noise level estimation method with application to EMD-based signal denoising," *J. Syst. Eng. Electron.*, vol. 27, no. 4, pp. 763–771, Aug. 2016.

[13] R. G. Wiley, *Electronic Intelligence: The Analysis of Radar Signals*. Dedham, MA, USA: Artech House, 1982, p. 250.

[14] H. Mardia, "New techniques for the deinterleaving of repetitive sequences," *IEE Proc. F, Radar Signal Process.*, vol. 136, no. 4, pp. 149–154, 1989.

[15] K. Nishiguchi and M. Kobayashi, "Improved algorithm for estimating pulse repetition intervals," *IEEE Trans. Aerosp. Electron. Syst.*, vol. 36, no. 2, pp. 407–421, Apr. 2000.

[16] Z.-M. Liu and P. S. Yu, "Classification, denoising, and deinterleaving of pulse streams with recurrent neural networks," *IEEE Trans. Aerosp. Electron. Syst.*, vol. 55, no. 4, pp. 1624–1639, Aug. 2019.

[17] H. Noh, S. Hong, and B. Han, "Learning deconvolution network for semantic segmentation," in *Proc. IEEE Int. Conf. Comput. Vis. (ICCV)*, Dec. 2015.

[18] J. Yang, S. E. Reed, M. Yang, and H. Lee, "Weakly-supervised disentangling with recurrent transformations for 3D view synthesis," 2016, *arXiv:1601.00706*. [Online]. Available: https://arxiv.org/abs/1601.00706

[19] A. Rasmus, H. Valpola, M. Honkala, M. Berglund, and T. Raiko, "Semi-supervised learning with ladder networks," in *Proc. Adv. Neural Inf. Process. Syst.*, 2015, pp. 3546–3554.

[20] K. Rematas, T. Ritschel, M. Fritz, E. Gavves, and T. Tuytelaars, "Deep reflectance maps," in *Proc. IEEE Conf. Comput. Vis. Pattern Recognit. (CVPR)*, Jun. 2016, pp. 4508–4516.

[21] R. G. Wiley, *ELINT: The Interception and Analysis of Radar Signals*. Norwood, MA, USA: Artech House, 2006.

[22] N. Ketkar, "Introduction to PyTorch," in *Deep Learning With Python*. Berkeley, CA, USA: Apress, 2017, pp. 195–208.